Hindawi
Shock and Vibration
Volume 2020, Article ID 7801085, 19 pages
https://doi.org/10.1155/2020/7801085

Research Article

Test on the Influence of Geometric Parameters of an Annular Trench on the Vibration Isolation Area

Jinglei Liu,[1,2] **Chuanqing Yu**,[1,2] **Kai Li**,[2] **Jie Liu**,[2] **and Mengyao Wen**[2]

[1]*Hebei Key Laboratory of Diagnosis, Reconstruction and Anti-Disaster of Civil, Zhangjia Kou 075000, China*
[2]*School of Civil Engineering, Hebei University of Architecture, Zhangjiakou 075000, China*

Correspondence should be addressed to Jinglei Liu; kingbest_1118@163.com

Received 1 November 2019; Revised 10 January 2020; Accepted 31 January 2020; Published 19 March 2020

Academic Editor: Franck Poisson

To study the influence of annular trenches on a vibration isolation area, the depth, width, vibration source distance, and central angle of the trench are analysed as research variables, and a contour diagram of the amplitude reduction ratio is drawn based on an outdoor test of the trench. Taking an area with an amplitude reduction ratio less than 0.40 as the evaluation index of the effective vibration isolation area, the effects of the above geometric parameters on the vibration isolation area are analysed. Limited to the test conditions of this paper, the results show that the depth, vibration source distance, and deep width ratio are the important factors affecting the effective vibration isolation area; with the increase of the above parameters, the effective vibration isolation area increases significantly, but the area increase rate decreases gradually. The width has a relatively little effect on the effective vibration isolation area. When the ratio of depth to width is from 7.05 to 9.15, and the width reaches 0.23 times the Rayleigh wavelength, the annular trench can have a good effective vibration isolation area. When the central angle of the trench is less than 90°, a discontinuous effective vibration isolation area will form in the vibration isolation region. The selection of the central angle of the trench is related to the frequency. With the same trench size, the effective vibration isolation area decreases as frequency decreases. In addition, the effect of distance depth ratio on the effective vibration isolation area presents a fluctuation. When the ratio of distance to depth is from 1.21 to 2.05, a good effective vibration isolation area can be obtained and it is reasonable.

1. Introduction

With the rapid urbanization of China, soil vibration caused by transportation, plant machinery, and construction interferes with the work and life of nearby residents and has an adverse effect on precision instruments and equipment. One of the methods for solving environmental vibration is to set up a vibration isolation barrier, which may be either continuous or discontinuous. For ideal geological soil layers, the continuous isolation barrier is commonly selected.

As a type of continuous isolation barrier, trenches have been studied by many experts and scholars, both domestic and abroad. Woods [1] first applied field tests to a trench, studied the influence of the ratio of the trench geometry parameter to the Rayleigh wavelength on the vibration isolation effect, and provided suggestions for the design of the trench. Haupt [2], Ahmad [3], and Liu [4] also performed trench vibration isolation tests to study the influence of geometric parameters on the vibration isolation effect. Yao [5] and Hu [6] used the theoretical analysis method to study the variation of the *R* wave passing through the trench. The results showed that the vibration-strengthening phenomenon will occur near the outer area of the trench. Using the wave function expansion method, Xu et al. [7, 8] studied the two-dimensional plane problem of the cellular cavity barrier to SV-wave isolation. The results showed that the vibration isolation effect near the edge of the barrier is better than that of the centre area. Then, the isolation of the P wave and SV wave is studied by using the same method. The results showed that the isolation area is obviously increased with the increase of the length of the trench. Using Biot fluid-saturated porous medium theory and a 2.5D indirect boundary element method, Ba et al. [9, 10] studied the vibration isolation effect of the trench on

vehicle-induced vibration in layered foundations. The results showed that the trench has a better vibration isolation effect on speed and acceleration than displacement. At the same time, with the increase of the train moving speed, the vibration isolation area becomes larger. Chen and Gao [11] used the 2.5D finite element method to study the vibration isolation effect of the filling trench on foundation vibration under irregular train dynamic load. The results showed that increasing the depth of the filling trench can improve the vibration isolation effect and expand the vibration isolation area. Liu [12] used the finite element method to study the effects of the trench and concrete underground continuous wall on the vibration isolation effect. The results showed that the trench can strengthen the vibration of the ground point in the first 2 m range and the trench has a good vibration isolation effect on the ground in the subsequent 45 m range, so the vibration isolation area of the trench is large. Gao et al. [13, 14] studied the effect of trench vibration isolation under a multilayer foundation using a thin layer method. The results showed that the trench can achieve a good vibration isolation effect associated with the upper-hard, soft-soft, or upper-soft-hard foundation. The delamination parameters have a great influence on the vibration isolation effect. The finite element method was used to study the vibration isolation effect of trench under high-speed train load and to analyze the influence of different geometric parameters of the trench on vibration isolation effect [15–18].

Most of the above research focuses on the analysis of the isolation effect of a rectangular trench and its influencing factors, but it rarely involves research related to the vibration isolation area and its influence parameters, and most of the research methods are theoretical analysis or finite element calculation. In view of the above problems, this paper takes the annular trench as the research object, adopts the test method to study the influence area of the annular trench vibration isolation effect, and analyses its depth, width, vibration source distance, and central angle in detail. The influences of depth and width, distance, and depth combination factors on the distribution of the vibration isolation area are discussed, and the relationship between the influence and the geometric parameters mentioned above is established, which provides suggestions for the design of annular trenches.

2. Site and Equipment

The test site is located away from urban areas in order to reduce artificial vibration and noise interference. The size of the test site is 4.0 m × 4.0 m × 2.0 m (length × width × depth). Considering that the soil parameters of the sandy soil are few and the test variables are easy to control, the in situ soil is replaced with the homogeneous sandy soil. At the same time, in order to reduce the interference of the boundary effect of the test site to the test results, the sandy soil layer is filled and tamped so that its density is maintained at 1.70 g/cm^3 to 1.80 g/m^3 and the moisture content is maintained at 12~13%. These values are basically consistent with those of the in situ soil. The physical properties of the back-filled sand in the test site are shown in Table 1. The cumulative curve of the sandy soil grain size distribution at the test site is shown in Figure 1. The composition of particles and related indices are shown in Table 2.

The WS-Z30 vibration table control system, which consists of a signal generator, an electromagnetic exciter, a charge amplifier, a power amplifier, and an accelerometer (sensitivity of 4 PC/ms^{-2}, frequency response of 0.2~8000 Hz, measuring range of 50 m/s^2, and mass of 28.5 g), data acquisition controller, accelerometer amplifier, etc. are used for the test. The test site and some of the test equipment are shown in Figure 2.

3. Test Procedure

The layout of the test site equipment is shown in Figure 3. The AB axis is a straight line parallel to the centre line of the test site. The exciter is arranged on the surface of the AB straight-line soil and acts as a point vibration source. The annular trench is arranged between the centre of the exciter and the trench, and it is symmetrically located around AB. The radius of the trench is set to 100 cm. Because the annular trench is symmetrical around the straight line of AB, half of the trench vibration isolation region is chosen as the test area. To accurately measure the variation of Rayleigh waves through the annular trench, the test used 10~12 accelerometers as a group, each of which was centred on an exciter and fixed at an angle of 5° between the groups, for a total of nine groups. The relative position of each sensor to the vibration source is shown in Figure 3.

The complex vibrations can be transformed into a sine wave by Fourier transform, and the sine wave has the characteristics of the simple waveform, stable signal, ease of control, and so on. Therefore, the frequency [19, 20] uses 30 Hz, 60 Hz, and 120 Hz sine waves as the excitation signals. The electromagnetic exciter can output the specified frequency and type of vibration wave such that the above-mentioned signal is generated by the exciter in the test. The sampling frequency is set to 5000 Hz, and the time is 3 s. The values of the charge amplifier are maintained to be consistent at all times. The parameters of the annular trench involved in the test are detailed in Table 3.

4. Evaluation Indicators

4.1. Evaluation Index of the Vibration Isolation Effect. Each test condition is repeated three times, and the average value of the time-domain curve acceleration amplitude is chosen as the vertical acceleration of the point. In this test, the surface amplitude reduction ratio (Ar) is used as the evaluation index to measure the vibration isolation effect. The Ar expression shows that the smaller the Ar value is, the better the vibration isolation effect is, as shown by

$$Ar = \frac{a_1}{a_0}, \tag{1}$$

where a_1 is the vertical acceleration value of the corresponding measurement point when the annular trench is set

Table 1: Physical index of the back-filled sand.

Index	Apparent density (kg/m^3)	Bulk density (kg/m^3)	Porosity (%)	Mud content (%)	Fineness modulus
Value	2621.8	1571.3	37.1	0.67	3.15

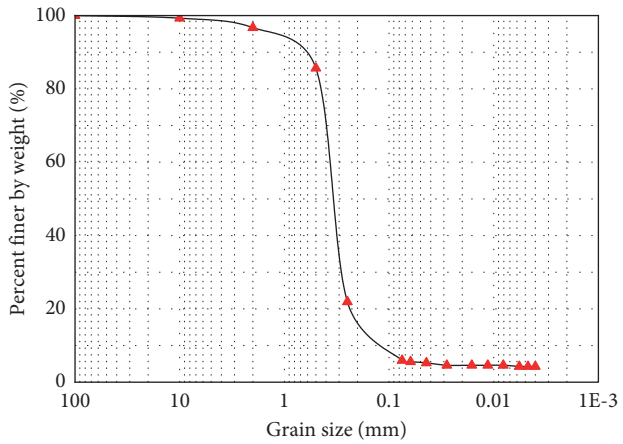

Figure 1: Grain size distribution curve.

Table 2: Particle composition and related indices of the back-filled sand.

Soil particle group name	Particle size range (mm)	Content (%)	Particle composition index	
Pebble	>60	—	d_{60}	0.368
	60~20	—		
Gravel	20~5	0.7	d_{30}	0.289
	5~2	2.6		
	2~0.5	11.1	d_{10}	0.127
Sand	0.5~0.25	63.7		
	0.25~0.075	16.0	C_u	2.9
	0.075~0.05	0.5		
Silt	0.05~0.01	0.8		
	0.01~0.005	0.4	C_c	1.9
Clay	0.005~0.002	>0.0		

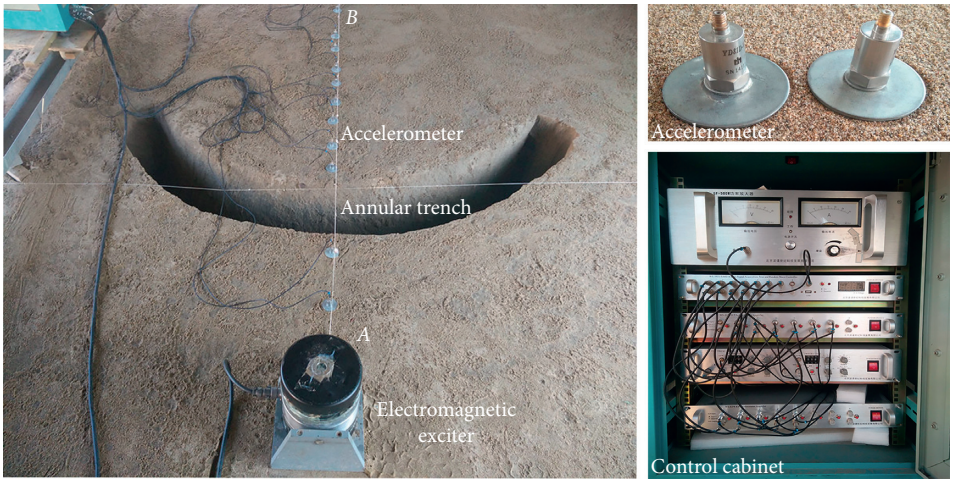

Figure 2: Test site and instruments.

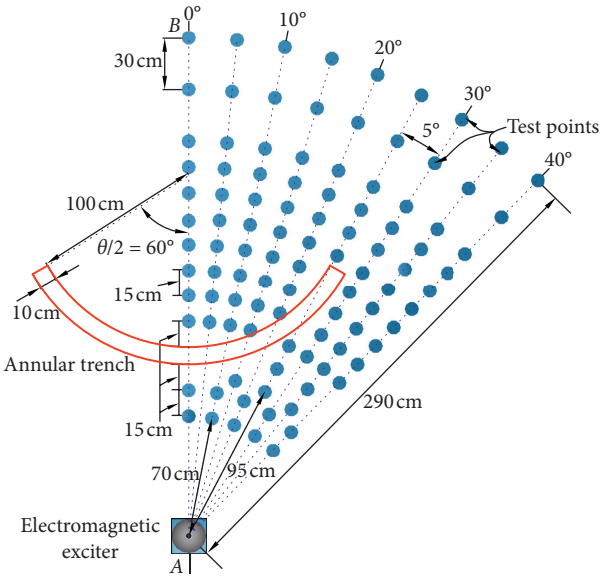

Figure 3: Test layout.

Table 3: Schedule of parameters for the annular trench.

Depth d (cm)	Width w (cm)	Source distance l (cm)	Central angle θ (degrees)
30	10	60	90
50	20	100	120
70	30	140	150
90	40	180	180

and a_0 is the vertical acceleration value of the corresponding measurement point when there is no trench.

4.2. Parameter Analysis Indicators. To study the influence of annular trench size and vibration source distance on the vibration isolation area, the following parameters are introduced to analyse and evaluate the trench.

4.2.1. Depth Parameter D. The ratio of the annular trench depth d to the Rayleigh wave wavelength λ_R is D, which indicates the physical quantity of the influence of trench depth on its vibration isolation area. The formula is

$$D = \frac{d}{\lambda_R}, \tag{2}$$

where d is the depth of the annular trench and λ_R is the Rayleigh wave wavelength.

4.2.2. Width Parameter W. The ratio of the annular trench width w to the Rayleigh wave wavelength λ_R is W, which indicates the physical quantity of the influence of trench width on its vibration isolation area. The formula is

$$W = \frac{w}{\lambda_R}, \tag{3}$$

where w is the width of the annular trench and λ_R is the Rayleigh wave wavelength.

4.2.3. Distance Parameter L. The ratio of the annular trench source distance l to the Rayleigh wave wavelength λ_R is L, which indicates the physical quantity of the influence of the trench position on its vibration isolation area. The formula is

$$L = \frac{l}{\lambda_R}, \tag{4}$$

where l is the distance between the trench and the vibration source and λ_R is the Rayleigh wave wavelength.

4.2.4. Deep Width Ratio Parameter S. The ratio of the annular trench depth d to the width w is S, which indicates the physical quantity of the influence of the depth and width on its vibration isolation area. The formula is

$$S = \frac{d}{w}, \tag{5}$$

where d is the depth and w is the width of the annular trench.

4.2.5. Distance Depth Ratio Parameter K. The ratio of the annular trench source distance l to the depth d is K, which indicates the physical quantity of the influence of the distance and depth on its vibration isolation area. The formula is

$$K = \frac{l}{d}, \tag{6}$$

where l is the distance and d is the depth of the annular trench.

5. Rayleigh Wave Velocity Measurement

The Rayleigh wave velocity was measured by the spectrum analysis method of the surface wave [21]. The #1 and #2 accelerometers are arranged on the ground of the test site, and under the action of the excitation load, the Rayleigh wave is first transmitted from the vibration source to the #2 accelerometer through the #1 accelerometer and continues to propagate outward. By using the spectrum analysis method, the mutual power spectrum and the coherent function spectrum of the two signals can be obtained. The phase difference generated by the time lag of the wave in the propagation process can be obtained in the mutual power spectrum, and the quality of the signal on the frequency band can be evaluated by using the coherence function. The coherence function is close to 1 in a certain frequency band, indicating that signal 1 and signal 2 have a good correlation in the frequency band; if the correlation function value is greater than 0.85 [22] in the test, it can be regarded as good coherence. That is, the #1~#2 accelerometers receive the same wave. Figure 4 shows the layout of the field Rayleigh wave velocity measurement accelerometer. Details of the wave velocity test analysis can be found in the study of Liu et al. [4].

The time t required for Rayleigh waves to travel from the #1 to the #2 accelerometer can be calculated according to the phase difference, as shown by

$$t = \frac{\varphi}{(360f)}, \tag{7}$$

where t is the time, φ is the phase difference, and f is the frequency.

The distance X between the two accelerometers is known, and the waves pass in turn through the #1 and #2 accelerometers, such that the Rayleigh wave velocity is calculated as shown in

$$V_R = \frac{(360Xf)}{\varphi}, \tag{8}$$

where V_R is the Rayleigh wave velocity and X is the distance between the #1 and #2 accelerometers.

According to the relationships between wave velocity, frequency, and vibration wavelength, the wavelength of the Rayleigh wave at different frequencies can be obtained:

$$\lambda_R = \frac{V_R}{f}. \tag{9}$$

The Rayleigh wave velocity can be obtained by substituting the test results into (7) and (8), for which the average value of the Rayleigh wave velocity is 109.99 m/s [4]. The Rayleigh wave wavelength can be calculated by substituting the Rayleigh wave velocity into (9). The maximum and minimum Rayleigh wave wavelengths are 3.67 m and 0.92 m, respectively.

6. Analysis of Test Results for Vibration Isolation Area

6.1. Influence of Depth on Vibration Isolation Area. To study the influence of the annular trench depth on the vibration isolation area, an annular trench with a width of 20 cm, a vibration source distance of 100 cm, and a central angle of 120° was used as the research object, and depth was used as a variable. The excitation frequencies of 30 Hz (low frequency), 60 Hz (medium frequency), and 120 Hz (high frequency) were used as variable conditions. The specific test conditions are shown in Table 4.

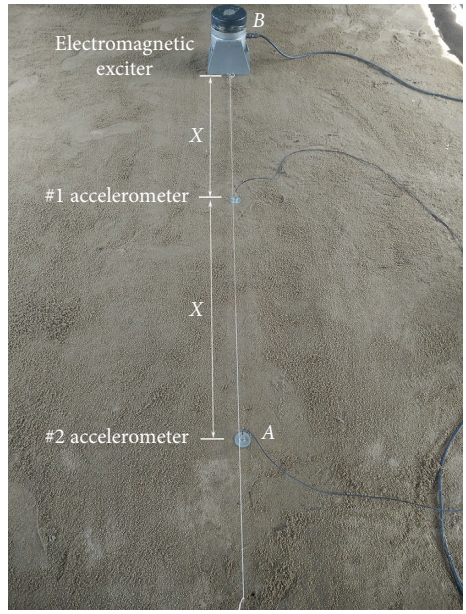

Figure 4: Layout of an accelerometer for the measurement of wave velocity.

The test conditions corresponding to low, medium, and high frequencies are comprehensively investigated. Taking the medium frequency of 60 Hz as an example, the 2D contours of Ar under other test conditions are only used for validation and comparison and are provided in this paper. The effect of deep vibration isolation is analysed by selecting test conditions 1-5 through 1-8 in Table 4. A two-dimensional contour diagram of Ar values is shown in Figure 5. The annular trench is placed in the AB line of the data acquisition area at the distance of the exciter (100 cm), and the arrangement of the accelerometer corresponds to that in Figure 3. Figure 5 marks S_1 and S_2 as two arcs with the centre of the exciter as the centre of the circle for analysis, which is not repeated in the following section.

Xu [7, 8] using a vibration isolation effect of 40% as an example analysed the influences of geometric parameters of a rectangular trench on the vibration isolation area. In this paper, the annular trench is used as the vibration isolation barrier, and area with Ar values of 0~0.40 in the vibration isolation area is regarded as the effective vibration isolation area (i.e., the area with 60% of the vibration isolation effect). The effective vibration isolation area is used to analyse the influence of the annular trench on the distribution of the effective vibration isolation area.

According to test conditions 1-5 through 1-8, the contour map of Ar in the data acquisition area produced some changes that are reflected in the following three observations: First, a sector-shaped effective vibration isolation area

Table 4: Test arrangement of the parameter *d*.

Test conditions	Excitation frequency (Hz)	*D*
1-1	30	0.08
1-2		0.14
1-3		0.19
1-4		0.25
1-5	60	0.16
1-6		0.27
1-7		0.38
1-8		0.49
1-9	120	0.33
1-10		0.55
1-11		0.76
1-12		0.98

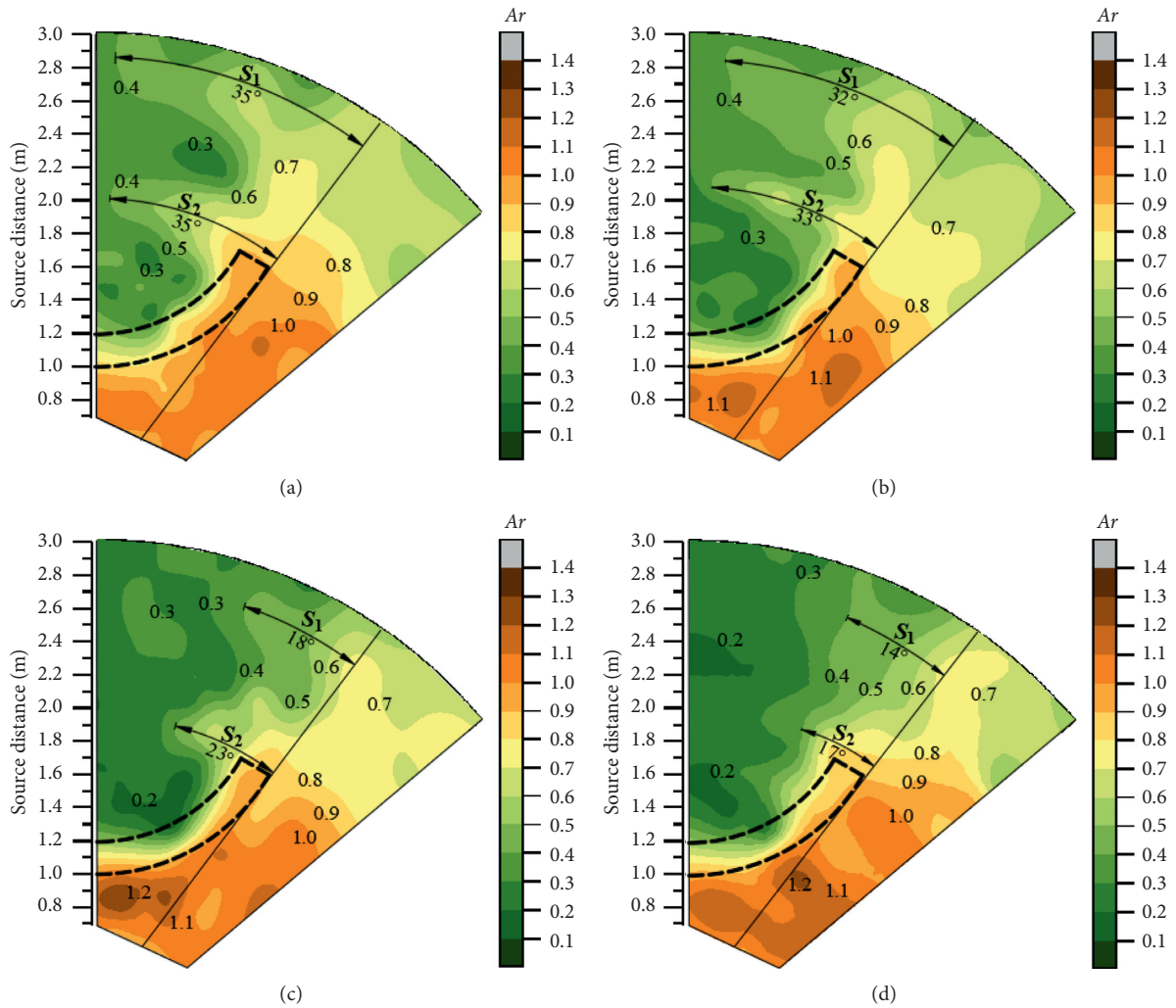

Figure 5: Amplitude reduction ratio contour map for test conditions (a) 1-5, (b) 1-6, (c) 1-7, and (d) 1-8.

is formed with the AB axis in the vibration isolation region. In the effective vibration isolation area, in which the *Ar* value ranges from 0 to 0.40, the annular trench shows a certain effect of vibration isolation. At the same time, when the *D* value increases from 0.16 to 0.49, the area of the effective vibration isolation region increases gradually and the angle of the effective vibration isolation region of the S_2 position increases by 18°. This indicates that the effective vibration isolation area can be increased by increasing the depth. Second, the positions of S_1 and S_2 are two vibration-

strengthening bands, and as depth increases, the areas of the two vibration-strengthening bands decrease. Finally, there is an obvious area of vibration enhancement located outside the annular trench and near the end of the trench, and the vibration of the soil in the above area is stronger than it is in the surrounding area. The reason for the occurrence of the vibration-strengthening area is that the propagation path of the surface Rayleigh wave is hindered by the trench, and the Rayleigh waves formed due to diffraction along the trench and gathered in the vibration isolation area.

For further analysis, we analysed the influence of the change in depth on the area of the effective vibration isolation region. In this paper, the area ratio η is introduced to describe the relative variation of the area of the effective vibration isolation region, as defined by

$$\eta = \frac{A_{0.4}}{A_S}, \tag{10}$$

where $A_{0.4}$ is the area of the effective vibration isolation region (that is, the area inside the annular trench isolation area where the Ar value is between 0 and 0.40) and A_S is the area inside the trench vibration isolation area.

Thus, the effective vibration isolation area is obtained earlier, as shown in Table 5. A fitting curve of the regression equation is drawn, as shown in Figure 6. Figure 6 shows as the D value increases, the η value also increases; when the D value is less than 0.38, the η value increases by 0.29, which means when the depth of the annular trench increases, the effective vibration isolation area increases significantly. When the D value is 0.38~0.68, the value of η increases by 0.11, and the area of the effective vibration isolation region continues to increase but at a slower rate. When the D value is 0.68~0.98, the η value increases by 0.07, and the area of the effective vibration isolation region changes mildly. The collected data are sorted and fitted. Under different test conditions, the relationship between D and η is shown as

$$\begin{aligned} \eta &= 0.19 \ln D + 0.72, \\ R^2 &= 0.85. \end{aligned} \tag{11}$$

According to the above analysis, the depth of the annular trench is an important parameter that affects the distribution of the effective vibration isolation area. The effective vibration isolation area can be significantly increased by increasing the depth, but at a slower rate, with the increase of the depth.

6.2. Influence of Width on Vibration Isolation Area. To study the influence of the annular trench width on the vibration isolation area, an annular trench with a depth of 50 cm, an angle of 120°, and a vibration source distance of 100 cm was used as the research object, and the width was variable. Similar to the depth test arrangement, the excitation frequencies of 30 Hz (low frequency), 60 Hz (medium frequency), and 120 Hz (high frequency) were used as contrasting conditions. The specific test conditions are shown in Table 6.

In this paper, the medium frequency of 60 Hz is taken as an example to illustrate the problem, and the contour diagrams of other test conditions are used for validation and comparison, which are not shown in this paper. Taking test conditions 2-5 through 2-8 in Table 6 as an example, the effects of width vibration isolation are analysed. A two-dimensional contour diagram of Ar is shown in Figure 7. The contour diagram of test condition 2-6 is shown in Figure 5, for condition 1-6.

For test conditions 2-5 through 2-8, the variation in width has the same effect on the two-dimensional contour diagram of Ar. The first is the vibration isolation effect: the effective vibration isolation area is formed over a certain range after the trench, and the area of the effective vibration isolation region gradually increases as the width increases. Second, the vibration enhancement area has the same influence on the vibration isolation area as the depth. The vibration enhancement area is located outside of the trench and at the end of the trench, and it extends to the vibration isolation area. This is mainly due to the diffraction of the Rayleigh wave as influenced by the width on the vibration isolation region, which is the same as the influence of the depth on the vibration isolation area. The vibration enhancement area exists to different degrees in the following tests and is basically the same as the distribution of the depth test, which is not repeated in the following section. Unlike the influence of the depth parameter on the vibration isolation area, the influence of the width parameter is different. First, at the position of S_2 in the vibration isolation area, as shown for test condition 2–5, an angle of 35° vibration reinforcement band appears, and the Ar value is greater than 0.4. The reason for this is due to Rayleigh waves passing through the bottom of the trench. Second, when the depth is constant, the width can be increased; thus, the area of the effective vibration isolation region increases, as shown by test condition 2-8. This is because increasing the width of the trench reduces the diffraction of Rayleigh waves at the bottom of the trench.

In the same way as for the depth analysis, the effect of width on the effective vibration isolation area is analysed using the area ratio η. The effective vibration isolation area is shown in Table 7. The collected data are sorted and fitted, and the fitting curve of the regression equation is drawn, as shown in Figure 8.

As shown in Figure 8, as the W value increases, the η value increases. When W is less than 0.13, the η value increases by 0.15, and the effective vibration isolation area can be increased significantly by increasing the width of the trench. When W is between 0.13 and 0.23, the value of η increases by 0.05. At this time, the area of the effective vibration isolation region of the trench continues to increase, but the rate of increase is relatively small. When W is between 0.23 and 0.33 and between 0.33 and 0.43, the respective values of η increase by 0.03 and 0.03. In this case, the area of the effective vibration isolation region increases continuously, but the effect is not obvious. Under different test conditions, the correlation between W and η is shown as

Table 5: List of vibration isolation areas.

Test conditions	1-1	1-2	1-3	1-4	1-5	1-6	1-7	1-8	1-9	1-10	1-11	1-12
D	0.08	0.14	0.19	0.25	0.16	0.27	0.38	0.49	0.33	0.55	0.76	0.98
$A_{0.4}$ (m^2)	0.80	1.05	1.35	1.05	0.77	1.10	1.68	1.60	1.38	1.68	1.93	1.98
η	0.29	0.38	0.49	0.38	0.28	0.40	0.61	0.58	0.50	0.61	0.70	0.72

$A_{S,0.2} = 2.75\ m^2$, where 0.2 represents the width of the trench (m).

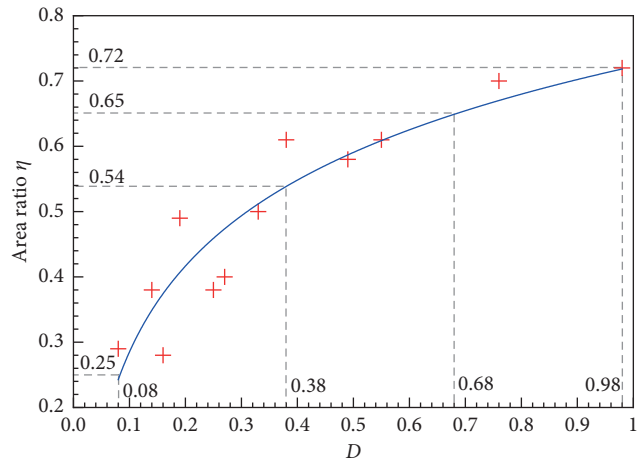

Figure 6: Fitting curve of D and η.

Table 6: Test arrangement of the parameter w.

Test conditions	Excitation frequency (Hz)	W
2-1	30	0.03
2-2		0.05
2-3		0.08
2-4		0.10
2-5	60	0.05
2-6		0.11
2-7		0.16
2-8		0.21
2-9	120	0.11
2-10		0.22
2-11		0.33
2-12		0.44

$$\eta = 0.13 \ln W + 0.71, \quad R^2 = 0.81. \tag{12}$$

This comprehensive analysis shows that the width of the annular trench has a certain effect on the distribution of the effective vibration isolation area. Limited to the test conditions in this paper, when W is greater than 0.23, a good effective vibration isolation area can be obtained.

6.3. Influence of Vibration Source Distance on Vibration Isolation Area. To study the influence of the vibration source distance on the vibration isolation area, an annular trench with a depth of 50 cm, a width of 20 cm, and an angle of 120° was used as the research object, and the distance was variable. Frequencies of 30 Hz (low frequency), 60 Hz (medium frequency), and 120 Hz (high frequency) were used as contrasting conditions, and specific test conditions are shown in Table 8.

In this paper, the medium frequency of 60 Hz is taken as an example to illustrate the problem, and the contour diagrams of other test conditions are used for validation, which is not shown in this paper.

Taking test conditions 3-5 through 3-8 in Table 8 as an example, the vibration isolation effect of the distance is analysed, and a two-dimensional contour map of Ar is shown in Figure 9. The contour diagram of test condition 3-6 is shown for test condition 1-6 of Figure 5. Compared to 3-5 through 3-8, modification of the vibration source distance has two effects on the two-dimensional contours of Ar. The first is the effect on the effective vibration isolation area: when the vibration source distance was small, the

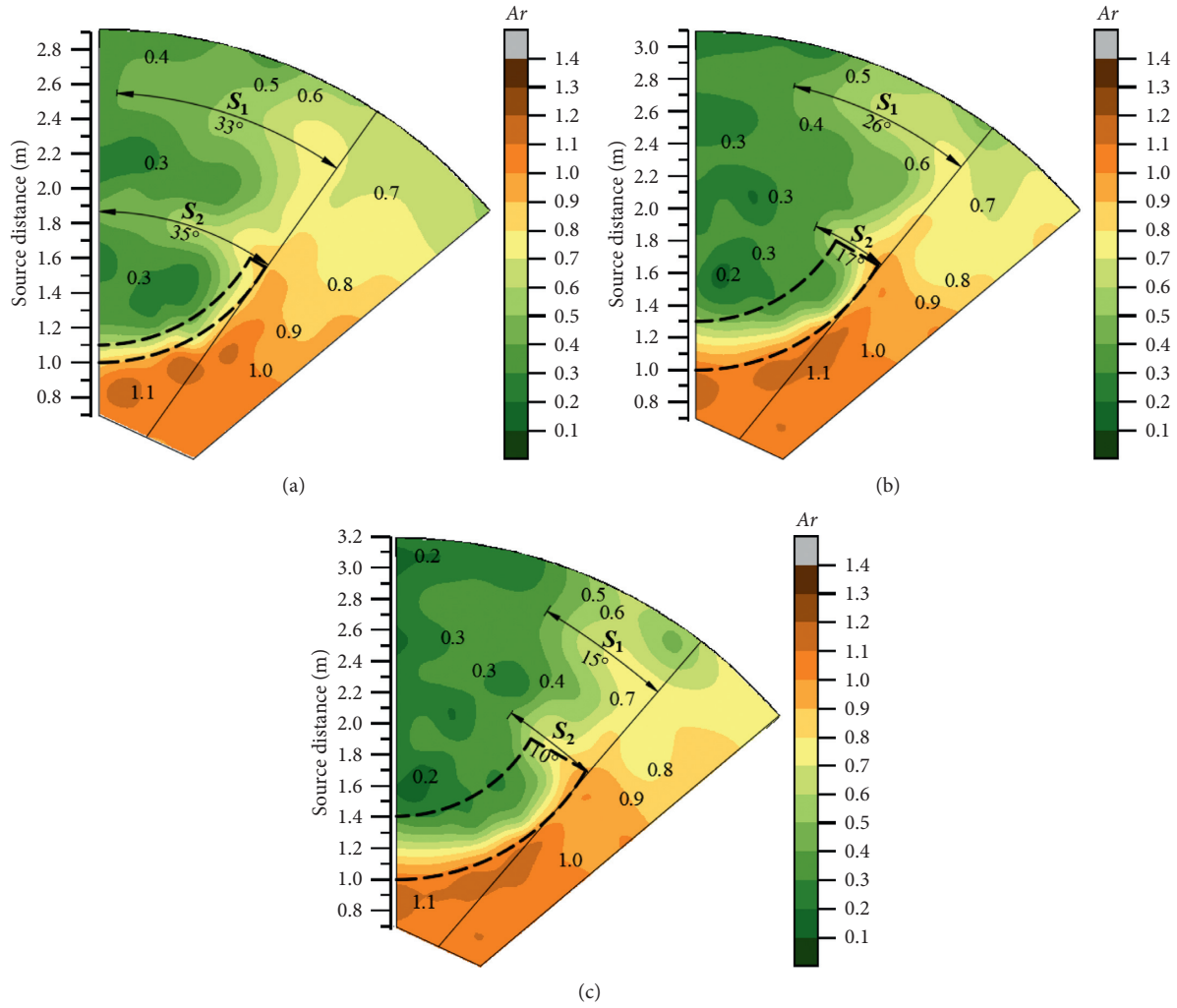

Figure 7: Amplitude reduction ratio contour map for test conditions (a) 2-5, (b) 2-7, and (c) 2-8.

Table 7: List of vibration isolation areas.

Test conditions	2-1	2-2	2-3	2-4	2-5	2-6	2-7	2-8	2-9	2-10	2-11	2-12
W	0.03	0.05	0.08	0.10	0.05	0.11	0.16	0.22	0.11	0.22	0.33	0.44
$A_{0.4}$ (m^2)	0.75	1.05	1.60	1.16	0.85	1.10	1.43	1.40	1.21	1.68	1.85	1.82
η	0.36	0.38	0.52	0.48	0.39	0.40	0.52	0.51	0.53	0.61	0.60	0.55

$A_{S,0.1} = 2.42\ m^2$, $A_{S,0.2} = 2.75\ m^2$, $A_{S,0.3} = 3.10\ m^2$, and $A_{S,0.4} = 3.31\ m^2$, in which 0.1, 0.2, 0.3, and 0.4 represent the width of the trench (m).

distribution of the effective vibration isolation area was discontinuous, as shown in Figure 9 (test condition 3-5). Two vibration-strengthening bands, S_1 and S_2, were formed in the vibration isolation area, and the effective vibration isolation area was divided into three parts. As the vibration source distance increased, the three effective vibration isolation areas gradually coalesced, which was due to the diffraction of the Rayleigh wave at the bottom and at the end of the trench when the vibration source was close to the trench. As the source distance increased, the number of Rayleigh waves passing through the trench decreased, as did the diffraction phenomenon at the end of the trench, which was accompanied by the consumption of Rayleigh wave energy. The second is the effect on the area of the effective vibration isolation region: by increasing the distance of the vibration source, the two vibration-strengthening bands S_1 and S_2 in the vibration isolation region gradually decreased, and the corresponding area of the effective vibration isolation region increased, as shown by test conditions 1-6, 3-7, and 3-8.

Further analysis of the area ratio η is also used to analyse the effect of distance on the effective vibration isolation area. The effective vibration isolation area is shown in Table 9. The data are fitted to a curve, as shown in Figure 10.

As L increases, the η value also increases, which indicates that the proportion of the effective vibration isolation area to the whole vibration isolation area increases

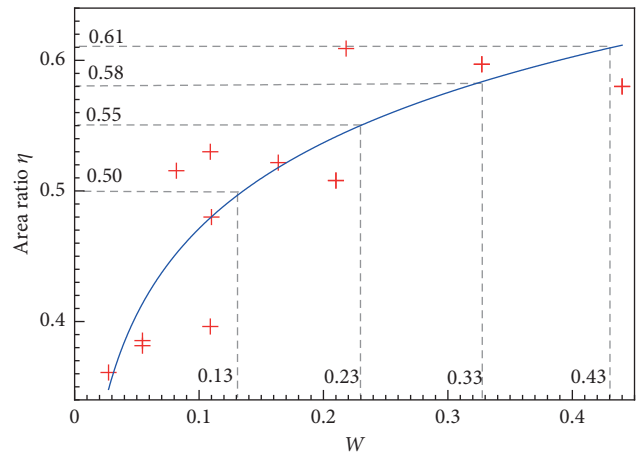

Figure 8: Fitting curve of W and η.

Table 8: Test arrangement for the parameter l.

Test conditions	Excitation frequency (Hz)	L
3-1	30	0.16
3-2		0.27
3-3		0.38
3-4		0.49
3-5	60	0.33
3-6		0.55
3-7		0.76
3-8		0.98
3-9	120	0.65
3-10		1.09
3-11		1.53
3-12		1.96

with the vibration source distance. When the L value is less than 0.61, the value of η increases by 0.19; in this case, the area of the effective isolation region can be increased significantly by increasing the distance of the vibration source. When L is between 0.61 and 1.06 and between 1.06 and 1.51, the respective values of η increase by 0.13 and 0.10. At this time, the effective vibration isolation area of the trench continues to increase, but the rate of increase is relatively small. When the L value is 1.51~1.96, the value of η increases by 0.08, and the area of the effective vibration isolation region does not increase obviously. Under different test conditions, the relationship between L and η is shown as

$$\eta = 0.55L^{0.44}, \quad R^2 = 0.77. \tag{13}$$

According to the above analysis, the distance of the vibration source has a great influence on the distribution of the effective vibration isolation area, and the area of the effective vibration isolation region can be obtained by increasing the distance of the vibration source, but at a slower rate, with the increase of the vibration source distance.

6.4. Influence of the Central Angle of Annular Trench on Vibration Isolation Area. To study the influence of the central angle of the annular trench on the vibration isolation area, a trench with a depth of 50 cm, a width of 20 cm, and a vibration source distance of 100 cm is chosen as the research object, and the central angle is variable. The excitation frequencies of 30 Hz (low frequency), 60 Hz (medium frequency), and 120 Hz (high frequency) are used as contrasting conditions. The specific test conditions are shown in Table 10.

In this paper, the medium frequency of 60 Hz is taken as an example to illustrate the problem, and the contour diagrams of other test conditions are used for validation, which is not presented in this paper. Taking test conditions 4-5~4-8 in Table 10 as an example, the two-dimensional contour diagram of Ar is shown in Figure 11, and the contour diagram of condition 4-6 is shown in Figure 5, condition 1-6.

Compared to test conditions 4-5~4-8, the change in the central angle of the annular trench has three effects on the effective vibration isolation area. First, as shown in test condition 4-4, two vibration-strengthening bands S_1 and S_2 with a 37° angle are formed in the vibration isolation area, which divide the effective vibration isolation area into three

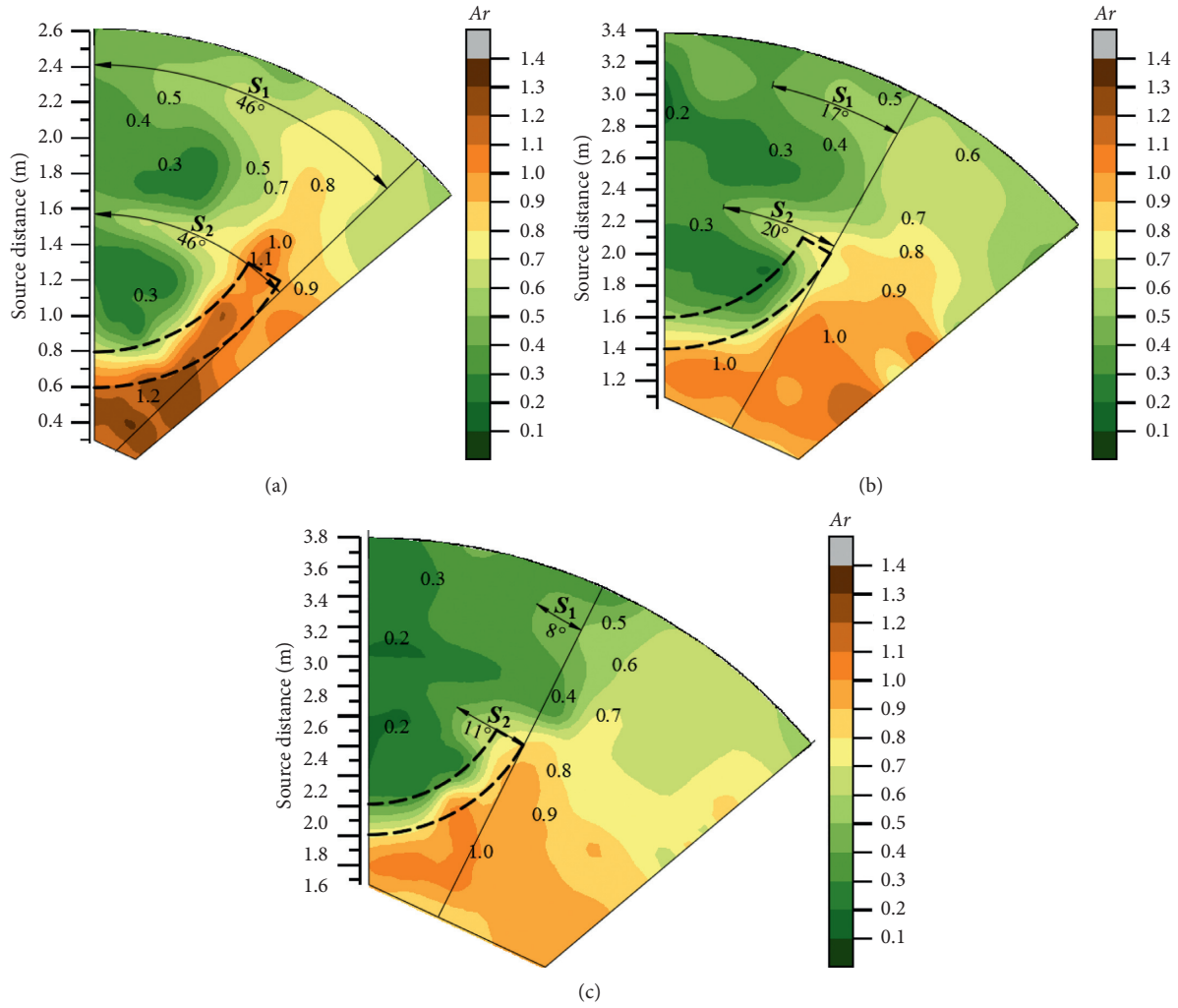

Figure 9: Amplitude reduction ratio contour map for test conditions (a) 3-5, (b) 3-7, and (c) 3-8.

Table 9: List of vibration isolation areas.

Test conditions	3-1	3-2	3-3	3-4	3-5	3-6	3-7	3-8	3-9	3-10	3-11	3-12
L	0.16	0.27	0.38	0.49	0.33	0.55	0.76	0.98	0.65	1.09	1.53	1.96
$A_{0.4}$ (m^2)	0.62	1.05	1.36	0.99	0.67	1.10	1.36	1.54	0.99	1.68	1.83	1.93
η	0.23	0.38	0.52	0.37	0.25	0.40	0.52	0.56	0.37	0.61	0.70	0.71

$A_{S,0.6} = 2.68\ m^2$, $A_{S,1.0} = 2.75\ m^2$, $A_{S,1.4} = 2.62\ m^2$, and $A_{S,1.8} = 2.72\ m^2$, where 0.6, 1.0, 1.4, and 1.8 represent the distance of source vibration (m).

discontinuous parts. As the central angle of the annular trench increases, the effective vibration isolation area gradually coalesces. Second, the area of the effective vibration isolation region is affected; as the central angle of the annular trench increases, the central angle of the vibration-strengthening bands S_1 and S_2 decreases. Corresponding to this, the effective vibration isolation area gradually increases. The variation in the above two aspects is due to the diffraction of the Rayleigh wave at the end of the trench. Finally, the effect of the central angle on the vibration-strengthening band is studied. When the angle is small, there are two vibration-strengthening bands S_1 and S_2 in the vibration isolation region, as shown by test condition 4-5. When the angle is increased, the two bands decrease to varying degrees. As the angle continues to increase, the vibration-strengthening band at the S_2 position decreases and ultimately disappears. The vibration-strengthening band at the S_1 position was in the process of decreasing, such as for test condition 4-8. The reason is mainly related to the diffraction ability of the Rayleigh wave at the end of the trench.

We further use the area ratio η to analyse the effect of the central angle on the effective vibration isolation area. The effective vibration isolation area is shown in Table 11. The collected data are sorted and fitted, and the fitting curve for the regression equation is drawn, as shown in Figure 12.

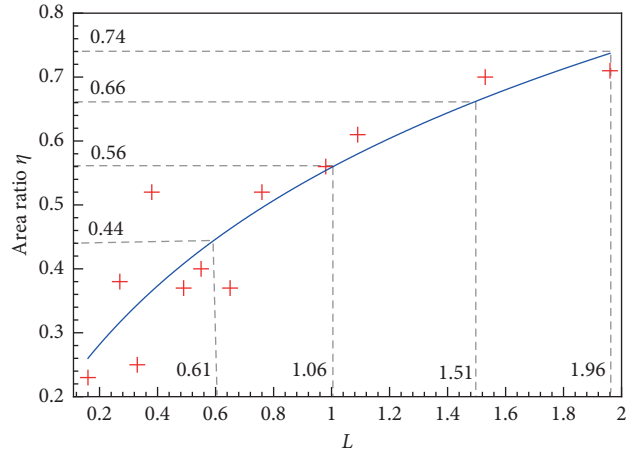

Figure 10: Fitting curve of L and η.

Table 10: Test arrangement for the parameter θ.

Test conditions	Excitation frequency (Hz)	Central angle θ (degrees)
4-1	30	90
4-2		120
4-3		150
4-4		180
4-5	60	90
4-6		120
4-7		150
4-8		180
4-9	120	90
4-10		120
4-11		150
4-12		180

Figure 12 shows three fitting curves of θ and η with different frequencies. The three curves have the same upward trend, with increasing θ and η values. This indicates that the area of the effective vibration isolation region can be increased significantly by increasing the central angle of the annular trench. In addition, the positions of the three fitting curves are different under different frequencies. As the frequency increases, the position of the fitting curve increases sequentially, which indicates that the effective vibration isolation area increases with the excitation frequency when the central angle of the trench is fixed. In other words, when the area of the effective vibration isolation region is constant, the central angle increases as frequency decreases. For example, when the excitation frequencies are 120 Hz, 60 Hz, and 30 Hz, the corresponding central angles of the trench are 110.22°, 138.10°, and 150°. The correlations between θ and η under the different test conditions are shown in Table 12.

In conclusion, the central angle of the annular trench is an important parameter that affects the distribution of the effective vibration isolation area. When the central angle of the trench is selected, an annular trench greater than 90° should be selected first. In addition, the selection of the central angle of the annular trench is related to the frequency; if the effective vibration isolation area is of the same size, the lower the frequency, the higher the central angle.

6.5. Influence of Deep Width Ratio on Vibration Isolation Area. To study the influence of the annular trench depth and width parameters on the vibration isolation area, an annular trench with a vibration source distance of 100 cm and an angle of 120° was used as the research object. Similar to the depth test arrangement, the specific test conditions are shown in Table 13.

The excitation frequencies of 30 Hz (low frequency), 60 Hz (medium frequency), and 120 Hz (high frequency) were used as contrasting conditions. In this paper, the medium frequency of 60 Hz is taken as an example to illustrate the problem, and the contour diagrams of other test conditions are used for validation, which is not presented in this paper.

Taking test conditions 5-1/4/8/12 in Table 13 as an example, the vibration isolation effect of S is analysed, and a two-dimensional contour map of Ar is shown in Figure 13. Compared to the above conditions, modification of the deep width ratio has the following effects on the two-dimensional

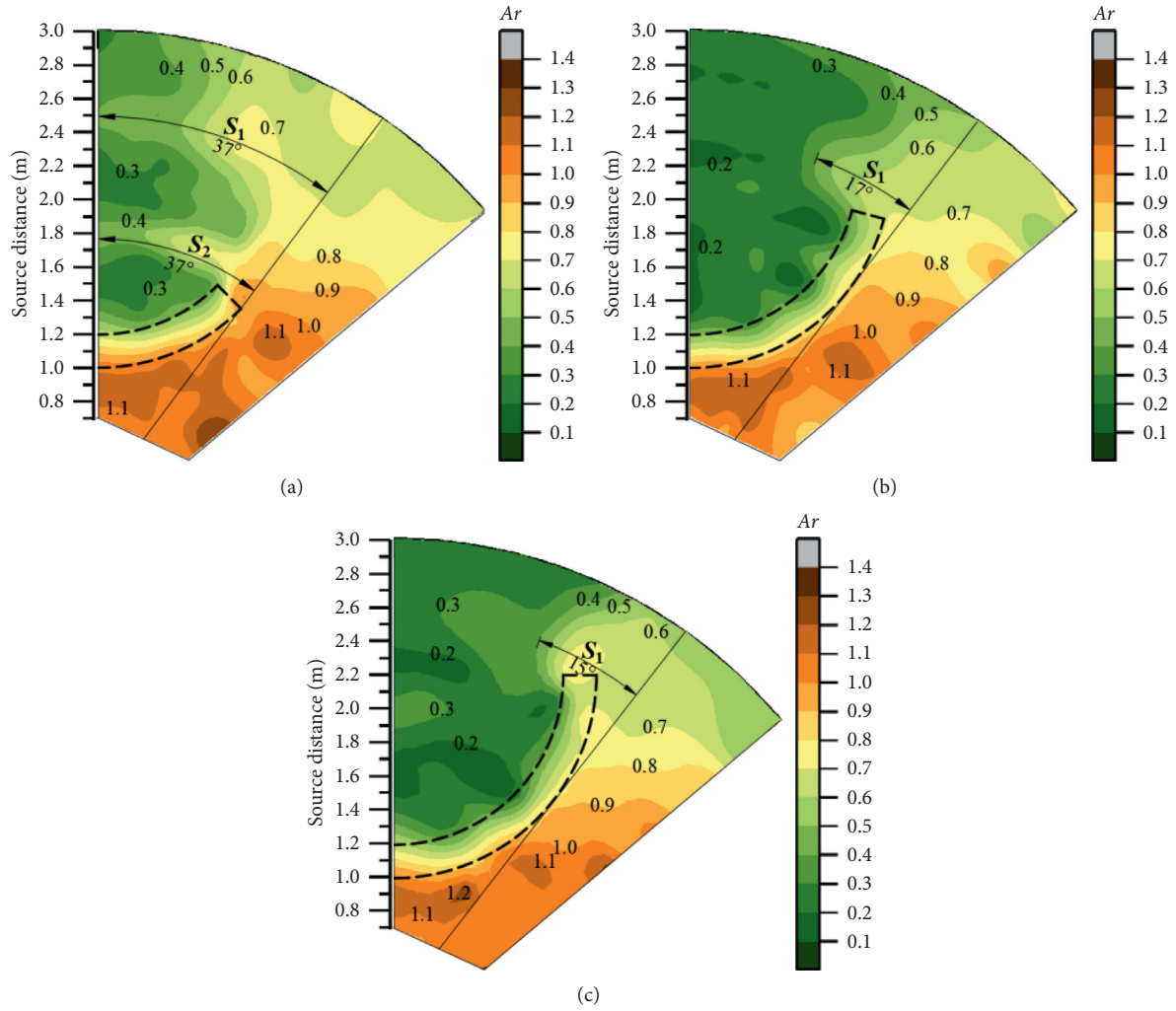

Figure 11: Amplitude reduction ratio contour map for test conditions (a) 4-5, (b) 4-7, and (c) 4-8.

Table 11: List of vibration isolation areas.

Test conditions	4-1	4-2	4-3	4-4	4-5	4-6	4-7	4-8	4-9	4-10	4-11	4-12
$A_{0.4}$ (m^2)	0.58	1.05	1.70	1.84	0.83	1.10	1.89	2.00	1.24	1.68	1.95	2.12
η	0.21	0.38	0.62	0.67	0.30	0.40	0.69	0.74	0.45	0.61	0.71	0.77

$A_{S,0.2} = 2.75\ m^2$, where 0.2 represents the width of the trench (m).

contours of *Ar*: When the deep width ratio is small, the distribution area of the effective vibration isolation region is small and irregular, as shown by test condition 5-1. As the deep width ratio parameter increases, the area of the effective vibration isolation region gradually increases, but they are discontinuous and cut by S_1 and S_2. As the deep width ratio parameter continues to increase, the area of the effective vibration isolation region gradually increases, and the connection becomes whole and it is continuously strengthened. The above analysis showed that when the ratio of depth and width is greater than a certain value, the annular trench can obtain a good and effective vibration isolation area.

Further analysis of the area ratio η is also used to analyse the effect of the deep width ratio on the effective vibration isolation area. The effective vibration isolation area is shown in Table 14. The data are fitted to a curve, as shown in Figure 14.

As *S* increases, the η value also increases, which indicates that the proportion of the effective vibration isolation area to the whole vibration isolation area increases with the deep width ratio. When the *S* value is less than 2.85, the value of η increases by 0.22; in this case, the area of the effective isolation region can be increased significantly by increasing the deep width ratio. When *S* is between 2.85 and 4.95 and between 4.95 and 7.05, the respective values of η increase by 0.09 and 0.06. At this time, the effective vibration isolation

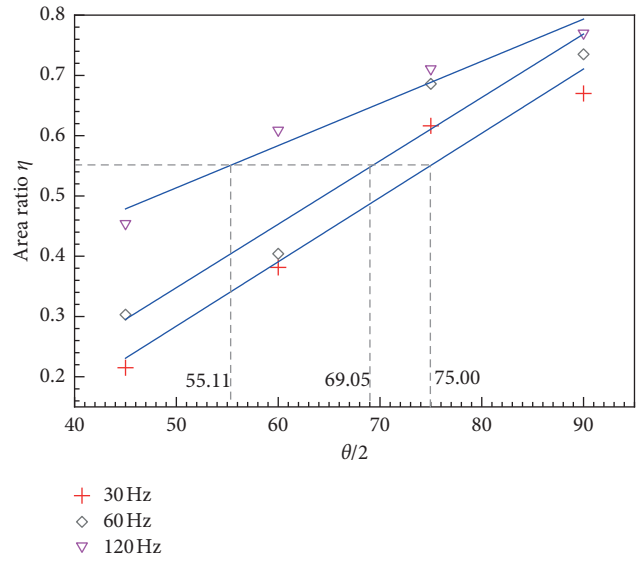

Figure 12: Fitting curve of θ and η.

Table 12: Correlation analysis of θ and η.

Test conditions	Comparison expression	R^2
4-1~4-4	$\eta = 0.01\theta - 0.35$	0.95
4-5~4-8	$\eta = 0.01\theta - 0.28$	0.93
4-9~4-12	$\eta = 0.01\theta + 0.16$	0.96

Table 13: Test arrangement for the parameter S.

Test conditions	d (cm)	w (cm)	S
5-1	30	40	0.75
5-2	30	30	1.00
5-3	30	20	1.50
5-4	70	40	1.75
5-5	90	40	2.25
5-6	70	30	2.33
5-7	50	20	2.50
5-8	90	30	3.00
5-9	70	20	3.50
5-10	90	20	5.00
5-11	70	10	7.00
5-12	90	10	9.00

area of the trench continues to increase, but the rate of increase is relatively small. When the S value is 7.05~9.15, the value of η increases by 0.03, and the area of the effective vibration isolation region does not increase obviously. Under different test conditions, the relationship between S and η is shown as

$$\eta = 0.16 \ln S + 0.32, \quad R^2 = 0.65. \tag{14}$$

According to the above analysis, the deep width ratio has a great influence on the distribution of the effective vibration isolation area, and the area of the effective vibration isolation region can be obtained by increasing the ratio of the depth to the width. Limited to the test conditions in this paper, when $S = 7.05$~9.15, a good effective vibration isolation area can be obtained.

6.6. Influence of Distance Depth Ratio on Vibration Isolation Area. To study the influence of the annular trench distance and depth parameters on the vibration isolation area, an annular trench with a width of 20 cm and an angle of 120° was used as the research object. Similar to the deep width ratio test arrangement, the specific test conditions are shown in Table 15.

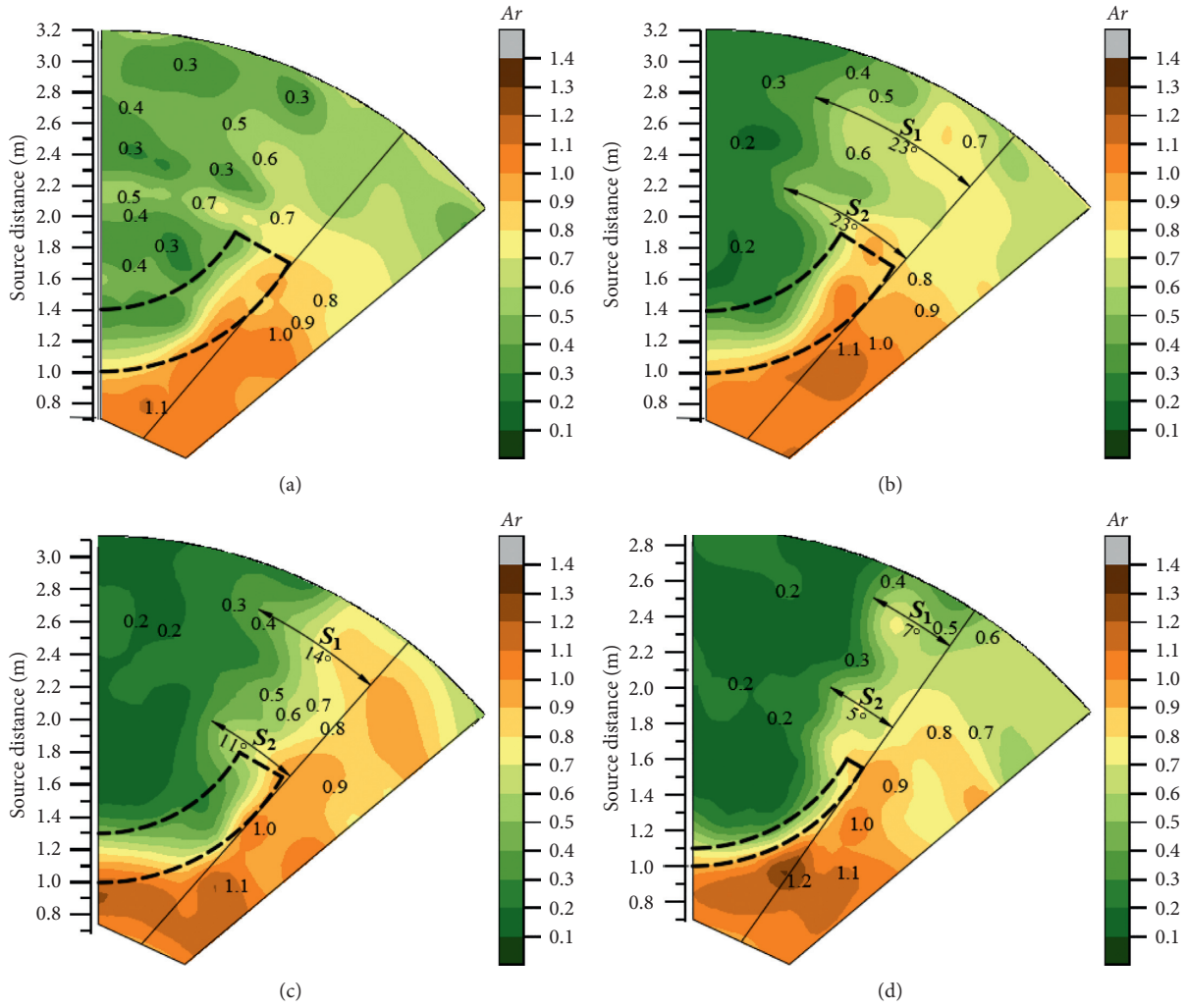

Figure 13: Amplitude reduction ratio contour map for test conditions (a) 5-1, (b) 5-4, (c) 5-8, and (d) 5-12.

Table 14: List of vibration isolation areas.

Test conditions	f (Hz)	$A_{0.4}$ (m^2)	η	f (Hz)	$A_{0.4}$ (m^2)	η	f (Hz)	$A_{0.4}$ (m^2)	η
5-1	30	0.66	0.20	60	0.73	0.22	120	1.00	0.30
5-2		0.79	0.25		0.78	0.26		1.02	0.33
5-3		0.80	0.29		0.77	0.28		1.38	0.50
5-4		1.29	0.39		1.49	0.45		1.52	0.46
5-5		1.42	0.43		1.59	0.48		1.56	0.47
5-6		1.64	0.53		1.41	0.46		1.74	0.56
5-7		1.05	0.38		1.10	0.40		1.68	0.61
5-8		1.71	0.55		1.80	0.58		1.74	0.56
5-9		1.35	0.49		1.68	0.61		1.93	0.70
5-10		1.04	0.36		1.09	0.39		1.43	0.53
5-11		1.47	0.61		1.51	0.63		1.57	0.65
5-12		1.48	0.61		1.57	0.65		1.68	0.69

$A_{S,0.1} = 2.42$ m^2, $A_{S,0.2} = 2.75$ m^2, $A_{S,0.3} = 3.10$ m^2, and $A_{S,0.4} = 3.31$ m^2, in which 0.1, 0.2, 0.3, and 0.4 represent the width of the trench (m); f represents the excitation frequency.

The excitation frequencies of 30 Hz (low frequency), 60 Hz (medium frequency), and 120 Hz (high frequency) were used as contrasting conditions. In this paper, the medium frequency of 60 Hz is taken as an example to illustrate the problem, and the contour diagrams of other test conditions are used for validation, which is not presented in this paper.

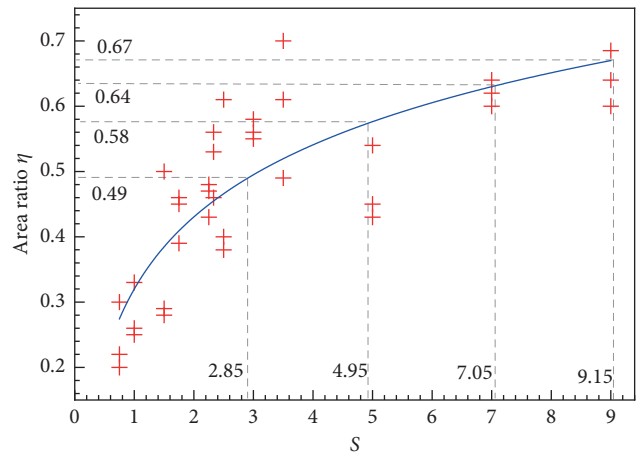

Figure 14: Fitting curve of S and η.

Table 15: Test arrangement for the parameter K.

Test conditions	l (cm)	d (cm)	K
6-1	60	90	0.67
6-2	60	70	0.86
6-3	60	50	1.20
6-4	100	70	1.43
6-5	140	90	1.56
6-6	180	90	2.00
6-7	180	70	2.57
6-8	140	50	2.80
6-9	100	30	3.33
6-10	180	50	3.60
6-11	140	30	4.67
6-12	180	30	6.00

Taking test conditions 6-1/5/9/12 in Table 15 as an example, the vibration isolation effect of K is analysed, and a two-dimensional contour map of Ar is shown in Figure 15. The contour diagram of test condition 6-9 is shown in Figure 5, for condition 1-5.

Compared to the above conditions, modification of the distance depth ratio has the following effects on the two-dimensional contours of Ar: When the distance depth ratio is small, a sector-shaped and continuous effective vibration isolation area is formed after the trench. As the distance depth ratio increases, the area of the effective vibration isolation region is continuously strengthened, as shown by test conditions 6-1 and 6-5. As the distance depth ratio continues to increase, two obvious vibration-strengthening bands S_1 and S_2 appear in the vibration isolation area, which divide the effective vibration isolation area. Finally, with the increase of the ratio, the two vibration-strengthening bands in the vibration isolation region gradually decrease. The above analysis shows that, with the increase of the distance depth ratio parameter, the effective isolation region goes through the process of firstly increasing, then decreasing, and finally gradually increasing.

Further analysis of the area ratio η is also used to analyse the effect of the distance depth ratio on the effective vibration isolation area. The effective vibration isolation area is shown in Table 16. The data are fitted to a curve, as shown in Figure 16.

As the distance depth ratio parameter increases, the area ratio changes in three stages: When K is less than 1.59, the η value increases with the increase of K, which indicates that the proportion of the effective vibration isolation area to the whole vibration isolation area increases with the distance depth ratio. When the K value is 1.59~4.62, the value of η decreases constantly, and the area of the effective vibration isolation region continues to decrease. When K is greater than 4.62, the η value increases with the increase of K, and at this time, the area of the effective vibration isolation region gradually increases. Under different test conditions, the relationship between K and η is shown as

$$\eta = 0.01K^3 - 0.16K^2 + 0.46K + 0.18, \quad R^2 = 0.53. \tag{15}$$

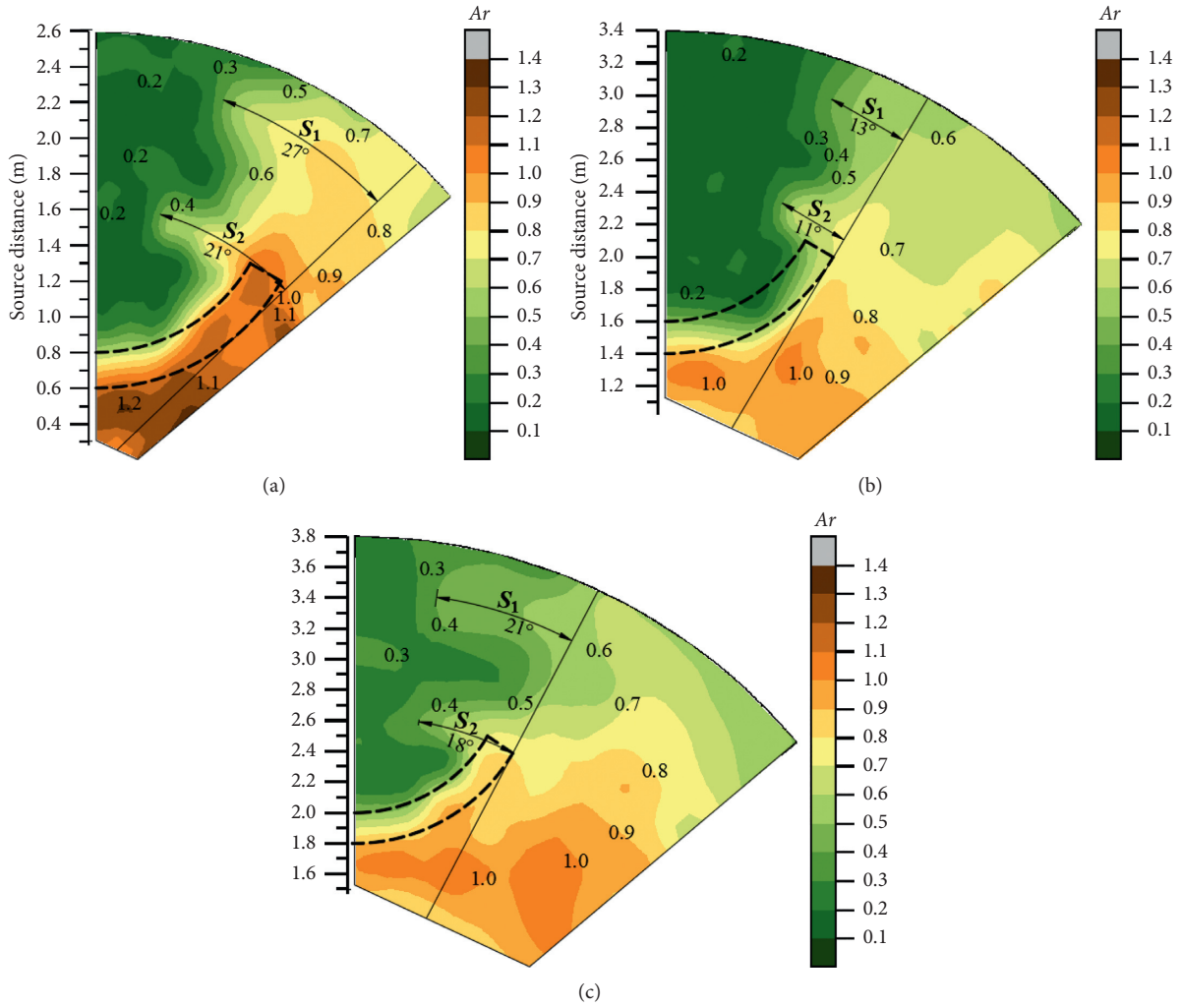

Figure 15: Amplitude reduction ratio contour map for test conditions (a) 6-1, (b) 6-5, and (c) 6-12.

Table 16: List of vibration isolation areas.

Test conditions	f (Hz)	$A_{0.4}$ (m^2)	η	f (Hz)	$A_{0.4}$ (m^2)	η	f (Hz)	$A_{0.4}$ (m^2)	η
6-1	30	1.10	0.41	60	1.38	0.52	120	1.52	0.57
6-2		1.21	0.45		1.10	0.41		1.22	0.46
6-3		1.15	0.43		1.21	0.45		0.99	0.37
6-4		1.35	0.49		1.68	0.61		1.93	0.70
6-5		1.59	0.61		1.65	0.63		1.70	0.65
6-6		1.68	0.62		1.77	0.65		1.87	0.69
6-7		1.55	0.57		1.58	0.58		1.73	0.64
6-8		1.36	0.52		1.36	0.52		1.49	0.57
6-9		0.80	0.29		0.77	0.28		1.38	0.50
6-10		1.01	0.37		1.52	0.56		1.83	0.67
6-11		0.84	0.32		0.84	0.32		1.00	0.38
6-12		0.93	0.34		0.96	0.35		1.12	0.41

$A_{S,0.6} = 2.68\ m^2$, $A_{S,1.0} = 2.75\ m^2$, $A_{S,1.4} = 2.62\ m^2$, and $A_{S,1.8} = 2.72\ m^2$, where 0.6, 1.0, 1.4, and 1.8 represent the distance of source vibration (m).

According to the above analysis, the distance depth ratio has a great influence on the distribution of the effective vibration isolation area, and in a certain range, the distance depth ratio is not bigger but better. Limited to the test conditions in this paper, when $K = 1.21 \sim 2.05$, a good effective vibration isolation area can be obtained by increasing the distance depth ratio.

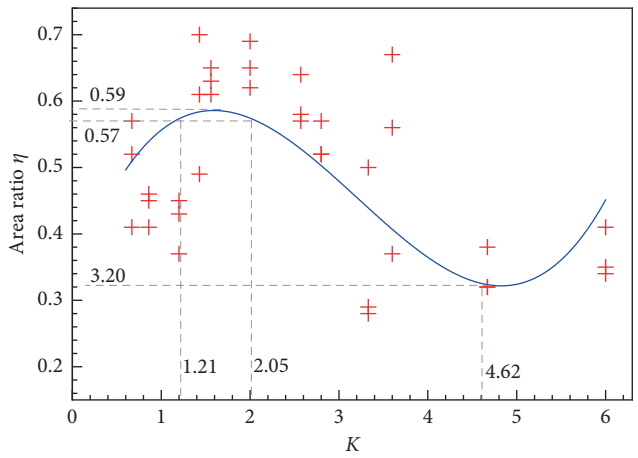

Figure 16: Fitting curve of K and η.

7. Conclusions

In this paper, a two-dimensional contour diagram of the amplitude reduction ratio of a test site is drawn via the method of outdoor tests, and the geometric factors that affect the distribution of the area are studied for an area of $Ar \leq 0.40$ (effective vibration isolation area). The main conclusions are as follows:

(1) The depth, width, vibration source distance, and central angle of the annular trench have certain influence on the distribution of the effective vibration isolation area. The geometric parameters mentioned above should be taken into account in the design of the trench.

(2) Increasing the depth of the trench can effectively reduce the diffraction of the Rayleigh wave at the bottom of the trench, resulting in the gradual connection of the effective vibration isolation area and an increase in the area of the effective vibration isolation region. When the width and vibration source distance are small, the effective vibration isolation area is divided into discontinuous parts. As width and the distance of the vibration source increase, the effective vibration isolation area becomes connected and is continuously strengthened. It is suggested that the width should be 0.23 times the Rayleigh wavelength, so a good effective vibration isolation area can be obtained. As the vibration source distance increases, the area increase rate decreases.

(3) Increasing the central angle can effectively reduce diffraction of the Rayleigh wave at the end of the trench, and the selection of a central angle is related to frequency. The lower the frequency, the higher the central angle when the effective vibration isolation area is achieved. A central angle greater than 90° should be prioritized; otherwise, a discontinuous effective vibration isolation area will be formed in the vibration isolation area.

(4) Increasing the ratio of depth to width, the area of effective vibration isolation region can be significantly increased. Limited to this test condition, when the S value is suggested to be 7.05~9.15, a good effective vibration isolation area can be obtained. The effect of the distance depth ratio on the effective vibration isolation area goes through a process of firstly increasing, then decreasing, and finally increasing again. It is suggested that the value of K is 1.21~2.05, which is more reasonable.

Data Availability

The data used to support the findings of this study are included within the article.

Conflicts of Interest

The authors declare that there are no conflicts of interest regarding the publication of this paper.

Acknowledgments

This project was supported by the Youth Talent Projects of Colleges in Hebei Province of China (No. BJ2016018). In addition, the Scientific and Technological Program of Research and Development of Zhangjiakou (1811009B-13) also supported this paper.

References

[1] R. D. Woods, "Screening of surface waves in soils," *Journal of the Soil Mechanics and Foundations Division*, vol. 94, no. 4, pp. 221–314, 1968.

[2] W. A. Haupt, "Model tests on screening of surface waves," in *Proceedings of the 10th International Conference in Soil Mechanics and Foundation Engineering*, vol. 3, pp. 215–222, Stockhoim, Sweden, 1981.

[3] S. Ahmad and T. M. Al-Hussaini, "Simplified design for vibration screening by open and in-filled trenches," *Journal of Geotechnical Engineering*, vol. 117, no. 1, pp. 67–88, 1991.

[4] J. L. Liu, C. Q. Yu, H. Liu et al., "Influence of geometric parameters of isolation trench on vibration isolation effect," *Journal of Vibration Engineering*, vol. 31, no. 6, pp. 930–940, 2018.

[5] J. B. Yao, H. Xia, and J. L. Hu, "Study on vibration isolation effect of open trench on environmental vibration induced by train operation," *China Railway Science*, vol. 39, no. 2, pp. 44–51, 2018.

[6] J. L. Hu, *Theoretical Research and Numerical Analysis of the Open Trench for Vibration Caused by Moving Train*, Beijing Jiaotong University, Beijing, China, 2016.

[7] P. Xu, "Analysis of vibration isolation effects of honeycomb-cell barriers," *Journal of Vibration and Shock*, vol. 33, no. 14, pp. 1–5, 2014.

[8] P. Xu, M. S. Shi, and C. J. Guo, "Theoretical analysis of isolation effects of an open trench on incident SH Waves," *Chinese Journal of Underground Space and Engineering*, vol. 11, no. 3, pp. 647–651, 2015.

[9] Z. N. Ba, J. W. Liang, and J. Y. Wang, "Isolation effect of an open trench against train induced vibration in a saturated layered ground," *Chinese Journal of Geotechnical Engineering*, vol. 39, no. 5, pp. 848–858, 2017.

[10] Z. N. Ba, J. Y. Wang, and J. W. Liang, "Reduction of train induced vibrations by using a trench in a layered foundation,"

Journal of Vibration Engineering, vol. 29, no. 5, pp. 860–873, 2016.

[11] G. Q. Chen and G. Y. Gao, "Vibration screening effect of infilled trenches on train dynamic loads of geometric irregular track in layered grounds," *Chinese Journal of Rock Mechanics and Engineering*, vol. 33, no. 1, pp. 144–153, 2014.

[12] Y. G. Liu, *Study on Environmental Vibration and Vibration Isolation Caused by High Speed Railway*, Southwest Jiaotong University, Chengdu, China, 2011.

[13] G. Y. Gao, Z. G. Peng, W. Li et al., "3D analysis of >active vibration isolation by open trench in layered ground PubMed/Crossref ReplacedPubmed Exact," *Northwestern Seismological Journal*, no. 3, pp. 210–220, 2006.

[14] G. Y. Gao, Z. G. Peng, M. F. Zhang et al., "Analysis of passive vibration isolation using open trench in layered ground," *Northwestern Seismological Journal*, vol. 31, no. 2, pp. 115–120, 2009.

[15] J. L. Liu, L. G. Zhang, and X. G. Song, "Numerical analysis and model test of vibration reduction by open trench on high speed railway," *Railway Standard Design*, vol. 61, no. 3, pp. 42–46, 2017.

[16] K. Chen, X. Jia, and B. Liu, "Finite element analysis of reducing the high speed railway vibration effect on the environment using open trenches," *China Earthquake Engineering Journal*, vol. 36, no. 3, pp. 575–579, 2014.

[17] D. J. Hou, X. Y. Lei, and X. W. Luo, "The numerical analysis of railway vibration reduction by trenches," *Journal of Railway Science and Engineering*, no. 2, pp. 48–52, 2006.

[18] Y. B. Yang, P. Ge, Q. Li, X. Liang, and Y. Wu, "2.5D vibration of railway-side buildings mitigated by open or infilled trenches considering rail irregularity," *Soil Dynamics and Earthquake Engineering*, vol. 106, pp. 204–214, 2018.

[19] J. L. Liu, G. S. Feng, J. Zhang et al., "Vibration isolation mechanism of concrete piles for Rayleigh waves on sand foundations," *Shock and Vibration*, vol. 2018, Article ID 6285491, 13 pages, 2018.

[20] J. L. Liu, G. S. Feng, J. H. Wang et al., "Model tests for effects of rail transits single row discontinuous vibration isolation barriers," *Journal of Vibration and Shock*, vol. 37, no. 11, pp. 175–182+201, 2018.

[21] Y. M. Chen, M. Wu, and G. X. Zeng, "Surface wave spectrum analysis method and its application," *Chinese Journal of Geotechnical Engineering*, no. 3, pp. 61–65, 1992.

[22] S. M. Wu, G. X. Zeng, Y. M. Chen et al., "Measurement of wave velocity of soil deposits by spectral analysis of surface waves," *Earthquake Engineering and Engineering Dynamics*, no. 4, pp. 27–32, 1988.